Effect of Ammonia on the Glutamate Dehydrogenase Catalyzed Oxidative Deamination of L-Glutamate. The Steady State†

Allister Brown,‡ Alan H. Colen, and Harvey F. Fisher*

ABSTRACT: Ammonia is known to inhibit the steady-state rate of oxidation of L-glutamate catalyzed by glutamate dehydrogenase. We reported previously [Brown, A., Colen, A. H., & Fisher, H. F. (1978) *Biochemistry 17*, 2031] kinetic evidence supporting the formation in the initial rapid phase of a complex which is composed of enzyme, reduced coenzyme, α-ketoglutarate, and ammonia. We show here that the effects of ammonia on the steady-state reaction can be correlated with transient-state kinetic effects related to the concentration of that ammonia-containing complex. These results indicate the existence of alternate reaction pathways which become important at high ammonia concentrations. These new pathways provide an additional route for the release of NADPH from the enzyme surface. The expanded mechanism shows that the noncompetitive product inhibition by ammonia can occur without the simultaneous presence of ammonia and L-glutamate on the enzyme. This mechanism also accommodates the observed substrate inhibition by L-glutamate.

The reversible oxidative deamination of L-glutamate catalyzed by glutamate dehydrogenase has been shown to be a multiphasic process at high enzyme concentration (Iwatsubo & Pantaloni, 1967; Fisher et al., 1970). The initial "burst" phase includes the hydride transfer step and results in the substantial loading up of active sites with reduced coenzyme–α-ketoglutarate complexes. The intermediate phase, where the observed absorbance changes only slightly, corresponds to the slow equilibration of reduced coenzyme–enzyme complexes. The final linear phase corresponds to the steady-state rate of L-glutamate oxidation (di Franco, 1974) and is correlated with the rates of dissociation of reduced coenzyme from the enzyme–reduced coenzyme complexes referred to above (di Franco & Iwatsubo, 1972; di Franco, 1974; Colen et al., 1975).

Several inhibitory complexes have been reported (Engel & Chen, 1975; Fisher & McGregor, 1960; Caughey et al., 1957). Of particular interest are the reports of product inhibition of the steady-state rate by ammonia.[1] The inhibition with respect to L-glutamate has been reported to be competitive (Fisher & McGregor, 1960). Engel & Chen (1975) reported noncompetitive inhibition at much lower coenzyme concentrations. Reasonable agreement is obtained for the inhibition constants (Engel & Chen, 1975; Fisher & McGregor, 1960) if allowance is made for the fact that ammonia produces an effect on each of the reported steady-state ϕ parameters (Engel & Chen, 1975). Understanding the precise function of ammonia as a product inhibitor and as a substrate is essential to the establishment of the mechanism for the glutamate dehydrogenase catalyzed oxidation of L-glutamate.

We have reported (Brown et al., 1978) kinetic evidence for an ammonia concentration dependent enzyme complex which is in equilibrium with the known (di Franco & Iwatsubo, 1972; Cross, 1972) enzyme–reduced coenzyme–α-ketoglutarate complex. In that report we discussed the kinetic changes, in the initial phase, produced by this intermediate. We report here the effect of this ammonia-dependent complex on the burst amplitude (the extent of reduced coenzyme formation in the initial rapid phase) and establish a relationship between the burst amplitude and the inhibition of the steady-state rate by ammonia. Tatemoto (1976) has reported a similar approach with alcohol dehydrogenase to establish the formation of a significant concentration of the ternary enzyme–coenzyme–substrate complex during the steady state.

Experimental Procedure

Description of the materials used and experimental details were given in the previous paper in this series (Brown et al., 1978). All experiments reported here are performed with 0.38 mM NADP and 0.018 mM glutamate dehydrogenase at 20 °C in 0.1 M potassium phosphate buffer, pH 7.6. The experimental wavelength is 320 nm. In each case, the reaction was initiated by mixing a solution containing enzyme, L-glutamate, and ammonium acetate with a solution containing enzyme and NADP in a Durrum-Gibson stopped-flow apparatus.

The initial steady-state velocities were calculated from changes in absorbance at 320 nm measured over the time increment 0.9–1.2 s, a total of 150 data points. The molar absorptivity for the enzyme–reduced coenzyme complexes (320 nm) at the end of the initial phase was taken to be 4.9 mM^{-1} cm^{-1} based on the spectrum for the enzyme–reduced coenzyme–α-ketoglutarate complex (Cross, 1972; di Franco & Iwatsubo, 1972).

Results

During the glutamate dehydrogenase catalyzed oxidation of L-glutamate, the addition of increasing concentrations of ammonia causes a marked decrease in the amplitude of the initial rapid burst of reduced coenzyme absorbance [as well as a corresponding increase in the observed rate constant (Brown et al., 1978)] and a decrease in the steady-state rate of appearance of reduced coenzyme absorbance.

The decrease in magnitude of the initial rapid absorbance change at 320 nm, the burst amplitude, with increasing con-

† From the Laboratory of Molecular Biochemistry at the Veterans Administration Medical Center, Kansas City, Missouri 64128, and the Department of Biochemistry of The University of Kansas School of Medicine. *Received April 4, 1977.* This work was supported in part by grants from the National Science Foundation (PCM78-26256) and from the General Medicine Institute of the National Institutes of Health (GM15188).

‡ Present address: C. D. Schultz and Co., Ltd., Vancouver, British Columbia, Canada V6E 3H4.

[1] The term "ammonia", as used in this paper, refers to all forms of ammonia in the solution: e.g., "ammonia concentration" means the sum of the concentrations of ammonium ion and free ammonia.

0006-2960/79/0418-5924$01.00/0

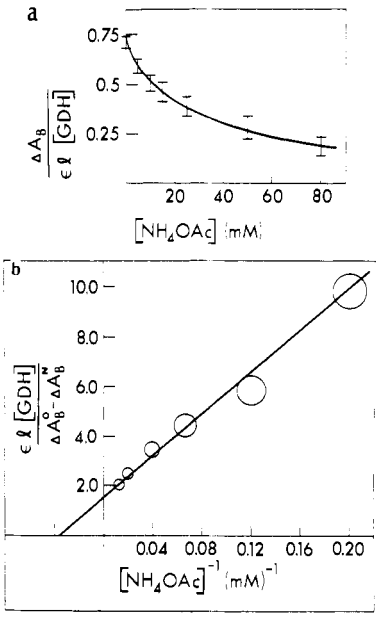

FIGURE 1: Effect of ammonium acetate concentration on burst amplitude at 25 mM L-glutamate. (a) A plot of mole fraction of enzyme–reduced coenzyme complexes formed in the initial rapid phase at several concentrations of ammonium acetate. (b) A double-reciprocal plot of the change in burst amplitude, $\Delta A_B^0 - \Delta A_B^N$, vs. ammonium acetate concentration. The change in burst amplitude is presented as mole fraction of enzyme. The superscripts 0 and N refer to burst amplitudes ΔA_B measured in the absence and presence of ammonia, respectively. See eq 1 for other definitions.

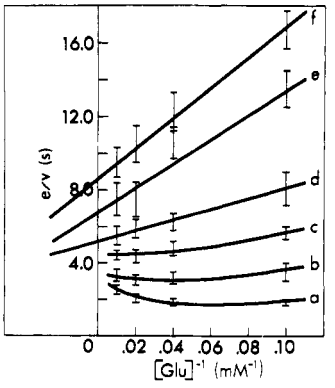

FIGURE 2: Double-reciprocal plot of initial steady-state velocity vs. glutamate concentration for several concentrations of ammonium acetate. Ammonium acetate concentrations are as follows: (a) 0, (b) 5, (c) 10, (d) 25, (e) 50, (f) 80 mM.

centration of added ammonium acetate is plotted in Figure 1 for 25 mM L-glutamate. This curved plot eventually reaches a point where any subsequent increase in the concentration of ammonium acetate will have a negligible effect on the burst amplitude as can be deduced from the magnitude of the nonzero intercept in the double-reciprocal plot of Figure 1b. The burst amplitude is controlled by the rates for the forward and reverse transformations occurring in this time range. These rates are proportional to the concentration of the complexes which are interconverting. Analysis of the ammonia concentration dependence of the burst amplitude gives a dissociation constant for ammonia, K_7 = 28 mM, in excellent agreement with the value determined kinetically (Brown et al., 1978). Thus, the decrease in burst amplitude of the 340-nm absorbance band is directly related to the ammonia concentration dependent intermediate reported previously.

The decrease in the steady-state velocity as a function of increasing concentration of added ammonium acetate is illustrated in Figure 2. Self-inhibition by glutamate is evident at the higher concentrations used in this study, but this effect decreases as added ammonium acetate increases. Quantitative analysis of these data is made difficult by the curvature produced by the self-inhibition of L-glutamate and the absence of data at lower L-glutamate concentrations. A plot of the reciprocal of steady-state velocity vs. added ammonium acetate concentration, Figure 3, is concave downward. The curvature is observed at all concentrations of glutamate used in this study, with deviations from linearity becoming pronounced at approximately 20 mM ammonium acetate. The following phenomena also become apparent at approximately 20 mM ammonium acetate. (1) Following the initial burst in reduced coenzyme absorbance, but preceding the steady-state phase, there occurs a shift in absorbance maximum (di Franco, 1974; Colen et al., 1975) which is most readily detected as a diminution of absorbance at 320 nm. This diminution can be evaluated by subtracting the increase in absorbance due to the steady-state oxidation as shown in Figure 4. For concentrations of ammonium acetate greater than or equal to 20 mM, this diminution in absorbance becomes difficult to detect. (2) It has also been reported (di Franco, 1974) that this shift in absorbance maximum is accompanied by an increase in reduced coenzyme fluorescence enhancement. We have confirmed this and find further that the fluoresence enhancement decreases as the concentration of added ammonium acetate

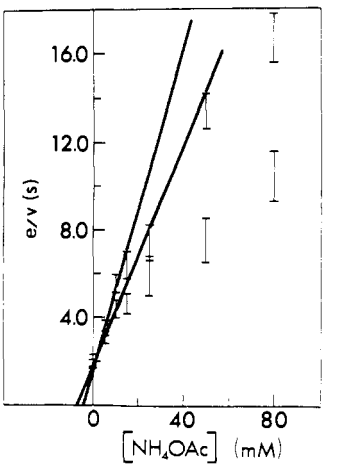

FIGURE 3: Inhibitory effect of ammonium acetate on the steady-state rate of oxidation of L-glutamate. Note the large deviation from linearity at moderate concentrations of ammonium acetate. The data shown are for [Glu] = 10 and 50 mM.

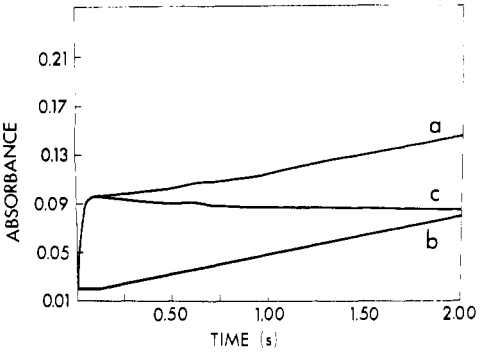

FIGURE 4: Illustration of the diminution in absorbance at 320 nm for enzyme–reduced coenzyme complexes during the rearrangement of ERK(N) to ER(G). Curve a is the data and curve b is the slope calculated for the steady-state velocity, for times longer than the initial phase. Curve c is the difference between curves a and b and illustrates the decrease in absorbance at 320 nm for enzyme–reduced coenzyme complexes upon rearrangement.

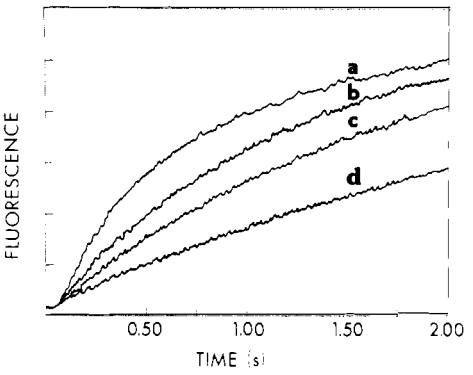

FIGURE 5: Reduced coenzyme fluorescence for the glutamate dehydrogenase catalyzed oxidation of L-glutamate. NH_4OAc concentration is (a) 0, (b) 10, (c) 20, and (d) 50 mM. The fluorescence enhancement observed in (a), at times of 0.1–1.0 s in the absence of ammonium acetate, decreases markedly with increasing concentration of ammonium acetate.

Scheme I

$$\begin{array}{ccccccc} EOG & \rightleftharpoons & ERK & \rightleftharpoons & ER & \rightleftharpoons & ERG \\ & & \downarrow\uparrow & & \downarrow\uparrow & & \downarrow\uparrow \\ & & EK + R & & E + R & & EG + R \end{array}$$

increases in the time range of our observations (see Figure 5).

Discussion

In a comprehensive study of the glutamate dehydrogenase catalyzed oxidation of L-glutamate, di Franco (1974) proposed the mechanism summarized in Scheme I. It should be noted that di Franco (1974) mentioned that the complex of enzyme, reduced coenzyme, and α-ketoglutarate, ERK, might also be enzyme, reduced coenzyme, either α-iminoglutarate or α-ketoglutarate, and ammonia. The latter complexes would be unidentifiable because their spectral properties are unknown. The proposed mechanism was supported by a correlation of the rate constants for each step of the catalytic reaction (di Franco, 1974) with rate constants for partial reactions measured in the absence of one or more of the substrates necessary for catalysis (di Franco & Iwatsubo, 1972). At high concentrations of L-glutamate, the complex of enzyme, reduced coenzyme, and L-glutamate, ERG, was reported to account for 80% of the total enzyme. Dissociation of reduced coenzyme from this complex is the major steady-state reaction pathway (di Franco, 1974) and thus considered to be rate limiting for L-glutamate oxidation. At low concentrations of L-glutamate, di Franco (1974) concluded that the rate of dissociation of α-ketoglutarate from the enzyme–reduced coenzyme–α-ketoglutarate complex, ERK, will limit enzyme turnover. These conclusions were supported by the data of Colen et al. (1975). Thus, the "rate-limiting step" in the steady state depends on the delicate balance of enzyme–reduced coenzyme complexes which in turn are governed by subtle changes in reactant concentrations. We have therefore sought to correlate the inhibition of the steady-state rate by ammonia with changes in concentration of ERK.

We have established previously (Brown et al., 1978) that the ammonia concentration dependent intermediate referred to in the introduction, ERKN, is on the reaction path and is in equilibrium with the complex ERK. Is it possible that the inhibition by ammonia of the steady-state rate of glutamate oxidation can be accounted for solely by including ERKN in the mechanism? This question is answered most directly by examining the changes in steady-state rate as a function of ERK concentration. The best measure of ERK concentration

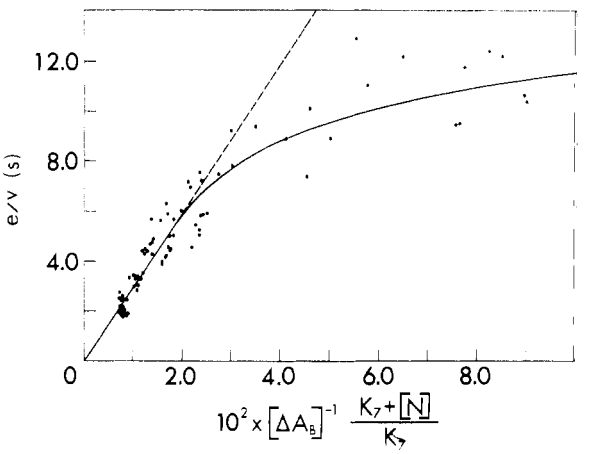

FIGURE 6: Double-reciprocal plot of initial steady-state velocity vs. the estimated concentration of ERK at the completion of the burst phase. To make this estimation, it is necessary to assume that the absorbance at 320 nm is due only to the complexes ERKN and ERK at the completion of the burst phase. K_7 was taken to be 45 mM (Brown et al., 1978).

comes from the burst amplitudes and is given as a function of ammonia concentration at the end of the first phase by eq 1.

$$[ERK] = \frac{\Delta A_B K_7}{[NH_4OAc] + K_7} \frac{1}{\epsilon l} \qquad (1)$$

In this equation ΔA_B is the absorbance change associated with the rapid initial phase of the reaction, K_7 is the dissociation constant for ammonia relating ERK and ERKN, ϵ is the molar absorptivity for ERK, and l is the cuvette path length. (The molar absorptivity for ERKN is unknown and is assumed to be equal to that of ERK.) The double-reciprocal plot of steady-state rate, v/e, vs. ERK concentration is shown in Figure 6 for all glutamate and ammonia concentrations used in this study. The points on this plot are experimental values. The self-inhibition by glutamate at 100 mM can be detected as slight upward displacements when little or no ammonia has been added (small ΔA_B^{-1}) (see Figure 6). The straight line and curved segments are shown only to indicate the trends. If the mechanism proposed by di Franco (1974), Scheme I, with the addition of ERKN could account for the inhibition by ammonia, the plot in Figure 6 should be linear. The curvature of this plot indicates that ammonia inhibition can not be accounted for simply by incorporating the complex ERKN into the reaction scheme. Furthermore, the curvature indicates that a step, previously undetected, makes a major contribution to the steady-state rate of oxidation of glutamate at higher concentrations of ammonia. This conclusion is further supported by the curvature of the plots in Figure 3, which indicates that the steady-state rate is faster than anticipated at high concentrations of ammonium acetate and that additional pathways for the dissociation of reduced coenzyme are very likely.

The additional step(s) in the steady-state rate cannot involve known dissociation processes of the complex ERK since all of these would give a linear plot in Figure 6. We clearly are looking for an alternate pathway for the dissociation of reduced coenzyme from the intermediate enzyme complexes. The inhibition by ammonia of the steady-state rate of glutamate oxidation by ammonia is readily explained by Scheme II.

Scheme II differs from Scheme I in the following ways. The ammonia dependent intermediate, ERKN, has been added. The pathway for dissociation of the reduced coenzyme from this intermediate, k_{21}, has been added. The product of this

Scheme II

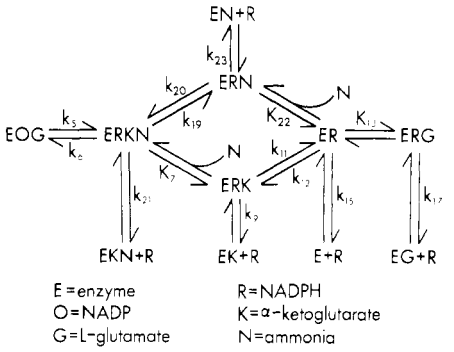

step is a complex which contains the elements of enzyme, α-ketoglutarate, and ammonia and may be the elusive enzyme–α-iminoglutarate complex reported by Hochreiter et al. (1972). The pathway for the dissociation of α-ketoglutarate from ERKN, K_{19}, to give ERN[2] has been added also. This pathway is phenomenologically indistinguishable from the direct dissociation of the elements of ammonia and α-ketoglutarate (α-iminoglutarate) to yield the complex ER. Both of these steps lead to the formation of complexes which exhibit fluorescence enhancement of reduced coenzyme and absorbance maxima which are slightly red-shifted. Direct measurement of these rate constants has not yet been reported. The rate expression for Scheme II is given by

$$\frac{1}{v} = \frac{\epsilon l}{\Delta A_B} \frac{[NH_4OAc] + K_7}{(k_{19} + k_{21})[NH_4OAc] + K_7(k_9 + k_{11})} \quad (2)$$

where ε is the appropriate molar absorptivity for the ERK and ERKN complexes, l is the cuvette path length, and ΔA_B is the absorbance change in the rapid initial phase. (The derivation of eq 2 and the expression for ΔA are given in the Appendix.) At low ammonia concentration, a linear dependence of e/v on ΔA_B^{-1} is expected. As ammonia concentration increases, partitioning between the complexes ERK and ERKN and the complexes ER and ERG shifts in favor of ERK and ERKN and is accomplished by a corresponding increase in magnitude of $(k_{19} + k_{21})[NH_4OAc]$. These changes lead to the curvature observed in Figure 6 and finally to a reciprocal velocity which is independent of added ammonia. The inclusion of these additional pathways (k_{19} and k_{21}) for dissociation of reduced coenzyme in the presence of ammonia appears to be sufficient to explain our observations. (The step represented by K_{19} does not involve directly the dissociation of reduced coenzyme from ERKN but rather the formation of ERN, a complex whose spectrum is indistinguishable from that of ER and ERG. The spectral phenomena described above indicate that the concentrations of such a complex are quite small even at high ammonia concentrations (up to 80 mM). This fact, however, does not rule out the possibility of a substantial flux through ERN and the equilibria represented by K_{22} and K_{23} to yield free R.)[3] The steady-state results reported by Engel & Dalziel (1969), who concluded that the reductive amination of α-ketoglutarate proceeds by a random mechanism for binding of substrates, provide further support for these pathways. It is interesting to note that eq 2 also accounts for the inhibition by L-glutamate seen in Figure 2. At high glutamate concentrations, $[G] > K_{13}$, the double-reciprocal plot in Figure 2 will deviate from linearity as the concentration of glutamate increases. (See eq 5, 6, 8, and 9 in the Appendix.)

The ammonia inhibition of the steady-state rate of glutamate dehydrogenase catalyzed oxidation of glutamate has been reported to be competitive (Fisher & McGregor, 1960) and noncompetitive (Engel & Chen, 1975); our results at high enzyme concentrations and high glutamate concentrations clearly indicate noncompetitive inhibition (Figure 2). The inhibition by ammonia, however, arises by a complex series of coupled events. Increasing the ammonia concentration increases the concentration of ERKN in Scheme II. This causes an increase in the rate of glutamate formation, k_6[ERKN], and decreases the concentration of the reduced coenzyme species at the end of the burst phase, a burst amplitude effect. Because the steady-state rate is controlled by the rate of dissociation of reduced coenzyme from the enzyme–reduced coenzyme complexes (di Franco, 1974; Colen et al., 1975), a decrease in burst amplitude alone might produce a noncompetitive inhibition if the only effect were to decrease the steady-state levels of the enzyme–reduced coenzyme complexes for the essentially ordered pathway proposed by di Franco (1974). However, the curvature in Figures 3 and 6 cannot be explained by this mechanism. When the concentration ratio [ERKN]/[ERK] was increased, the contribution of a second path for dissociation of reduced coenzyme must become increasingly significant. Inclusion of the alternate paths (k_{21} and k_{19}) will produce the noncompetitive kinetic patterns observed and will also account for the behavior in Figures 3 and 6.

It is interesting to speculate on the structure of the complex ERKN. It is not unlikely that this complex is composed of enzyme-bound α-iminoglutarate and does not contain any free ammonia. If this is the case, the inhibition by ammonia occurs without forming significant concentrations of an enzyme–ammonia encounter complex and is due only to an enzyme–α-iminoglutarate complex. In any event, the inhibition by ammonia can be accounted for without postulating the simultaneous binding of L-glutamate and ammonia, as suggested by Engel & Chen (1975). The inhibition arises because the inhibitory effect is directed at a step whose kinetic significance is masked in the steady-state initial rate studies. In the glutamate dehydrogenase reaction these steps may be unmasked by studying the rapid burst phase of the reaction with L-glutamate.

Appendix

During the steady-state phase of the oxidative deamination of L-glutamate, the complex ERKN equilibrates rapidly with ERK as does ER with ERG and probably with ERN. By application of the steady-state approximation to each group of protein complexes

$$\frac{d([ERKN] + [ERK])}{dt} = 0 \quad (3)$$

$$\frac{d([ERN] + [ER] + [ERG])}{dt} = 0 \quad (4)$$

the steady-state rate of dissociation of reduced coenzyme from

[2] Since no direct evidence has yet been produced for the existence of a stable ERN complex, N may dissociate nearly simultaneously with K, giving ER directly.

[3] One of us (A.B.) feels that "the ratio k_{21}/k_{19} would appear to be large, based on the time frame for spectral detection of the red-shifted, fluorescence-enhanced products" at high ammonia concentrations. A.C. and H.F., however, do not believe that the present experiments permit us to distinguish between the two paths because the known red-shifted, fluorescence-enhanced products equilibrate rapidly with free R and the retarded production of such complexes simply tracks the inhibition of the steady-state rate by ammonia.

all complexes is given by eq 5.

$$E_T/v = \left[(k_5' + k_6 + k_{19} + k_{21})\frac{[NH_4OAc]}{K_7} + k_5' + k_{11} + k_9 + k_5'\left(k_{11} + k_{19}\frac{[NH_4OAc]}{K_7} \right)B \right] \Big/ \left[k_5'\left[(k_{19} + k_{21})\frac{[NH_4OAc]}{K_7} + k_9 + k_{11} \right] \right] \quad (5)$$

where

$$B = \frac{1 + \frac{[G]}{K_{13}} + \frac{[NH_4OAc]}{K_{22}}}{k_{15} + k_{17}\frac{[G]}{K_{13}} + k_{23}\frac{[NH_4OAc]}{K_{22}}} \quad (6)$$

and

$$(k_5')^{-1} = \phi_0 + \frac{\phi_1}{[O]} + \frac{\phi_2}{[G]} + \frac{\phi_{12}}{[O][G]} \quad (7)$$

is the reciprocal specific initial velocity of the burst phase in the absence of ammonium acetate (Colen et al., 1972; Brown et al., 1978). Assuming that only ERK and ERKN complexes make a substantial contribution to the absorbance at the end of the burst phase, the burst amplitude is given by

$$\frac{\Delta A_B}{el} = \frac{[NH_4OAc] + K_7}{K_7}[ERK] \quad (8)$$

where

$$[ERK] = k_5'E_T/\left[(k_5' + k_6 + k_{19} + k_{21})\frac{[NH_4OAc]}{K_7} + k_5' + k_{11} + k_9 + k_5'\left(k_{11} + k_{19}\frac{[NH_4OAc]}{K_7} \right)B \right] \quad (9)$$

Combining eq 5–9 yields eq 2 in the text.

References

Brown, A., Colen, A. H., & Fisher, H. F. (1978) *Biochemistry 17*, 2031.

Caughey, W. S., Smiley, J. D., & Hellerman, L. (1957) *J. Biol. Chem. 224*, 591.

Colen, A. H., Wilkinson, R. R., & Fisher, H. F. (1975) *J. Biol. Chem. 250*, 5243.

Cross, D. G. (1972) *J. Biol. Chem. 247*, 784.

di Franco, A. (1974) *Eur. J. Biochem. 45*, 407.

di Franco, A., & Iwatsubo, M. (1972) *Eur. J. Biochem. 30*, 517.

Engel, P. C., & Dalziel, K. (1969) *Biochem. J. 115*, 621.

Engel, P. C., & Chen, S. S. (1975) *Biochem. J. 151*, 305.

Fisher, H. F., & McGregor, L. L. (1960) *Biochem. Biophys. Res. Commun. 3*, 629.

Fisher, H. F., Bard, J. R., & Prough, R. A. (1970) *Biochem. Biophys. Res. Commun. 41*, 601.

Hochreiter, M. C., Patek, D. R., & Schellenberg, K. A. (1972) *J. Biol. Chem. 247*, 6271.

Iwatsubo, M., & Pantaloni, D. (1967) *Bull. Soc. Chim. Biol. 49*, 1563.

Tatemoto, K. (1976) *Arch. Biochem. Biophys. 166*, 25.

Purification and Enzymatic Properties of Lysyl Hydroxylase from Fetal Porcine Skin†

Ronald L. Miller* and Hugh H. Varner, Jr.‡

ABSTRACT: Lysyl hydroxylase from fetal porcine skin is shown to bind in a highly specific manner to aminoethyl-Sepharose 4B. When coupled to ammonium sulfate fractionation and DEAE-cellulose chromatography, chromatography of lysyl hydroxylase preparations on aminoethyl-Sepharose 4B has yielded a highly purified (>95%) preparation of lysyl hydroxylase. The enzyme consists of two subunits with molecular weights of 70 000 and 115 000. The overall recovery of activity was 2.5%, yielding ~3.5 mg of purified enzyme from 900 g of fetal porcine skin. The enzyme is more active at 30 °C than at 37 °C and has a pH optimum near 8.0. Both catalase and bovine serum albumin are required by the enzyme for maximum activity. The sulfhydryl reagents *p*-(chloromercuri)-benzoate, *N*-ethylmaleimide, and iodoacetamide are potent inhibitors of the enzyme, whereas dithiothreitol appears to be an activator.

Collagen hydroxylysine and hydroxyproline residues are the result of posttranslational modification of the collagen polypeptides. Previous studies have demonstrated that these modifications of the collagen polypeptide are carried out by two separate enzymes, lysyl hydroxylase and prolyl hydroxylase (Miller, 1971; Kivirikko & Prockop, 1972; Popenoe & Aronson, 1972). Both of these enzymes require molecular oxygen, α-ketoglutarate, ferrous iron, and ascorbic acid as cofactors (Cardinale & Udenfriend, 1974). Further progress has been made in the purification of lysyl hydroxylase from chick embryos (Ryhänen, 1976; Turpeenniemi et al., 1977); however, it appears that the enzyme used in those studies was less than 40% pure. The hydroxylation of collagen lysine residues is a required prerequisite to the glycosylation of collagen (Butler & Cunningham, 1966) and to the formation of certain cross-link components that contain hydroxylysine residues (Tanzer, 1973; Barnes et al., 1971; Mechanic, 1972).

We wish to report the purification of fetal porcine skin lysyl hydroxylase to greater than 95% purity and some of the enzymatic properties of the enzyme. Relatively simple techniques

† From the Department of Biochemistry, Medical University of South Carolina, Charleston, South Carolina 29403. *Received April 20, 1979.* These studies were supported in part by National Institutes of Health Grant AM16767 and in part by a grant (RR 05767) from a State Appropriation for Biomedical Research.

‡ Present address: Laboratory of Developmental Biology and Anomalies, National Institute of Dental Research, National Institutes of Health, Bethesda, Md.

0006-2960/79/0418-5928$01.00/0